

# A nanoelectromechanical tunable laser

MICHAEL C. Y. HUANG, YE ZHOU AND CONNIE J. CHANG-HASNAIN\*

Department of Electrical Engineering and Computer Sciences, University of California at Berkeley, California 94720, USA

\*e-mail: cch@eecs.berkeley.edu

Published online: 24 February 2008; doi:10.1038/nphoton.2008.3

The ability to tune the frequency of an oscillator is of critical importance and is a fundamental building block for many systems, be they mechanical or electronic<sup>1,2</sup>. However, this very important function is still highly inadequate in optical oscillators, particularly in semiconductor laser diodes<sup>3,4</sup>. The limitations in tuning a laser frequency (or wavelength) include the tuning range and the speed of tuning, which is typically milliseconds or slower. In addition, the tuning is often not continuous and may require complex synchronization of several electrical control signals. In this Letter, we present a new tunable laser structure with a lightweight nanoelectromechanical mirror based on a single-layer, high-contrast subwavelength grating. The high-contrast subwavelength grating reflector enables a drastic reduction of the mirror mass, which increases the mechanical resonant frequency and hence tuning speed<sup>5</sup>. This allows for a wavelength-tunable light source with potential switching speeds of the order of tens of nanoseconds and suggests various new areas of practical application, such as bio- or chemical sensing<sup>6–8</sup>, chip-scale atomic clocks<sup>9</sup> and projection displays<sup>10,11</sup>.

A wavelength-tunable semiconductor laser has been constructed by combining an optical microelectromechanical (MEM) mirror<sup>12</sup> with a vertical-cavity surface-emitting laser (VCSEL)<sup>13,14</sup>. Their monolithic integration brings together the best of both technologies and leads to an unprecedented performance in wavelength-tunable lasers with simple electrical control<sup>15–17</sup>. The MEM-tunable VCSEL has a large proportion of its top mirror held on a micromechanical structure and is physically moved by means of electrostatic attraction. The physical movement changes the optical cavity length and thus produces a change in the lasing wavelength. The laser has two pairs of electric contacts, one for tuning the wavelength and the other for data modulation, which can be at data rates of  $\sim 10$  Gbit s<sup>-1</sup> (ref. 18). Such MEM-tunable VCSELs also offer the advantages of batch processing and wafer-level testing, both of which are essential for low-cost, high-volume manufacturing. However, because of the short gain medium, VCSELs often require distributed Bragg reflectors (DBRs) with a thickness of 3–6 times the optical wavelength in air to construct mirrors with sufficiently high reflectivity. Such DBRs could be as thick as 4  $\mu\text{m}$  and 10  $\mu\text{m}$  for VCSELs emitting at 850-nm and 1.55- $\mu\text{m}$  wavelengths, respectively. When integrating with MEM structures, these rather thick DBRs impose significant design limitations on the length and width of the mechanical actuators. Thus, the mass of the movable structures translates into a slow tuning speed, a limited tuning range, high actuation power, as well as epitaxy and processing difficulties.

Recently, we demonstrated the realization of a surface-emitting laser using an ultrathin (230 nm), high-contrast subwavelength

grating (HCG) reflector that overcomes the requirement for 30–40 pairs of DBRs in the VCSELs<sup>19,20</sup>. Experimentally, the device exhibits excellent optical performance, including low threshold current, moderate output power, deterministic polarization and single-mode emission. The HCG structure consists of a single layer of periodic subwavelength grating composed of a high-refractive-index material (for example, AlGaAs or Si) surrounded entirely by low-index material (for example, air or oxide)<sup>21,22</sup>. We now present a high-speed nanoelectromechanical optoelectronic (NEMO) tunable VCSEL by integrating the HCG with nanoscale actuators to create a mobile and lightweight reflector. The small footprint of the HCG enables scaling down of the mechanical actuating structure by at least a factor of ten in each of the dimensions, and thus the overall mass is less than one thousandth that of regular DBR-based photonic MEM devices, resulting in much lower power consumption and much faster tuning speed.

A schematic of the electrostatic-actuated NEMO-tunable VCSEL is shown in Fig. 1a. The device consists of an n-doped HCG top mirror, a cavity layer containing the active region, and a bottom standard n-doped DBR mirror on a GaAs substrate. The HCG is freely suspended above a variable air gap and supported by a nanomechanical structure (such as a cantilever, bridge, folded beam or membrane). Electric current injection is conducted through the middle laser contact (by means of two pairs of p-doped DBRs above the cavity layer) and backside contact (through the substrate). An aluminium oxide aperture is formed on an AlAs layer within the p-DBR section to provide current and optical confinement. The mechanical tuning contact is fabricated on the top n-doped HCG layer. Figure 1b shows a scanning electron microscope (SEM) image of a fabricated NEMO-tunable VCSEL with the HCG aligned to the oxide aperture in the mesa centre. Figure 1c shows the integration of the freely suspended HCG mirror with a variety of nanomechanical actuators that can be designed for different values of mechanical stiffness.

Continuous-wave operation of an electrostatic-actuated NEMO-tunable VCSEL with excellent optical performance has been demonstrated. Figure 2a shows the optical characteristics of a fabricated device, showing the output power and voltage versus bias current. The device exhibits a very low threshold current of 200  $\mu\text{A}$  and moderate output power of 0.5 mW when injected with 2 mA of current, with external slope efficiency 0.25 mW mA<sup>-1</sup>. Compared with a MEM VCSEL with similar epitaxy structure, but using a DBR-based movable top mirror (with a threshold current of  $\sim 1.2$  mA)<sup>23</sup>, both the reduction of threshold current and slope efficiency indicate that a much higher effective reflectivity is obtained by using the single-layer

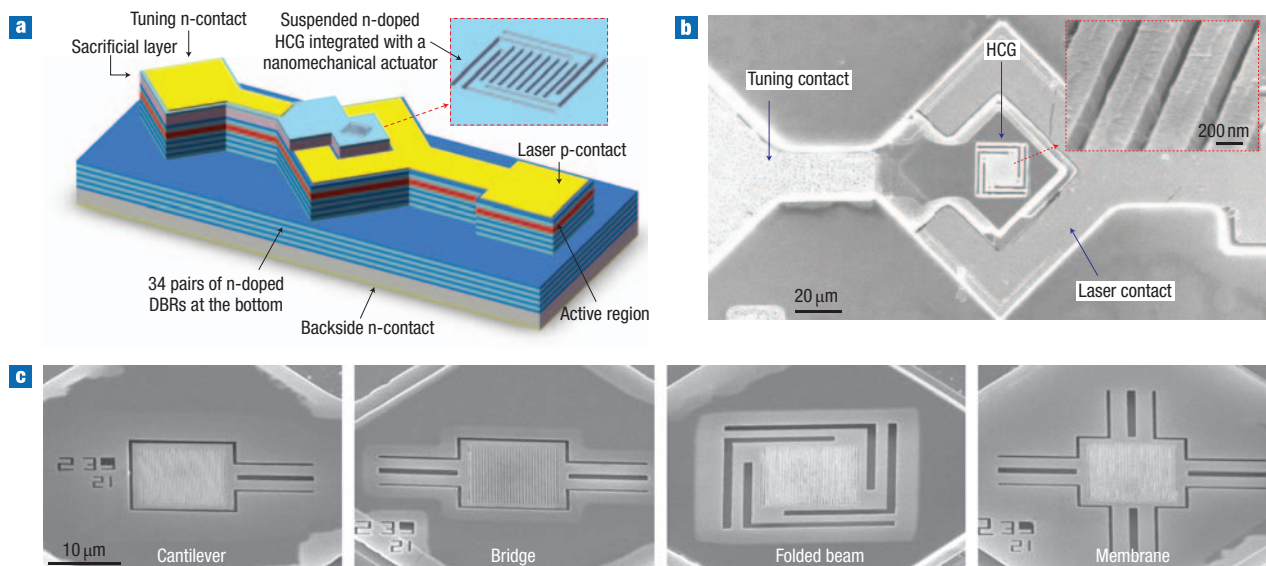


**Figure 1** Nanoelectromechanical tunable laser with a lightweight mirror. **a**, Schematic of a NEMO-tunable VCSEL using the highly reflective HCG as its top mirror, instead of conventional DBRs. **b**, Scanning electron microscope image of the fabricated NEMO-tunable VCSEL. The inset shows the freely suspended grating stripes. **c**, Scanning electron microscope images of the HCG mirror monolithically integrated with various mobile and lightweight nanomechanical actuators (cantilever, bridge, folded beam and membrane).

HCG top mirror, in addition to the reduction of free-carrier absorption loss. However, the ultrahigh reflectivity in the HCG leads to low threshold current, but also lower output power a reflectivity adjustment can be obtained by optimizing the grating parameters lithographically to maximize the VCSEL output power, but with a slightly higher threshold current. The measured device emission spectrum at 1 mA bias current is shown in the inset of Fig. 2a. Single-transverse-mode emission with a >40-dB side-mode suppression ratio is obtained, where the discrimination of higher-order transverse modes is attributed to the finite grating effects<sup>24</sup> in combination with the oxide aperture. Figure 2b illustrates the near-field optical characteristics of the emission beam from the laser. Despite the grating having a rectangular structure, the optical emission output remains a symmetrical, fundamental-mode gaussian profile. The beam diameter is measured to be about 3  $\mu\text{m}$ , which is characterized by the width of the 99% drop in intensity.

Wavelength tuning of the NEMO-tunable VCSEL is accomplished by applying a reverse voltage bias across the tuning contact and the laser contact, while a constant electrical current is applied between the laser and backside contact. The reverse bias across the p-i-n junction results in a negligibly small leakage current of  $\sim 10$  nA, which does not affect the operation of the VCSEL current injection. Figure 3a shows the measured wavelength-tuning spectra of a fabricated NEMO VCSEL, where the mobile HCG mirror is integrated with a bridge nanomechanical actuator. The device is electrically pumped at  $\sim 1.2$  times the threshold current and actuated under various applied voltages across the tuning contact. An 8-nm continuous wavelength tuning towards the shorter wavelength is first obtained within 0–6 V of external applied voltage. The NEMO VCSEL stops lasing when the external applied voltage is further increased, as the optical loss becomes larger than the laser gain. When the voltage reaches 9 V, the device starts lasing again, but at another longitudinal mode, and continuously tunes again for 13 nm over the applied voltage range of 9–14 V. With the total

spectral overlap, an overall continuous wavelength tuning range of 18 nm is experimentally obtained. Figure 3b shows the experimentally measured threshold current and slope efficiency of the NEMO VCSEL under the corresponding tuning wavelengths, indicating the increased optical loss when the laser wavelength is tuned towards both edges of the tuning spectrum. Finally, because of the weight reduction of the mechanical actuator, an ultralow actuation power <100 nW is required to tune the emission wavelength, which is 500–1,000 times less power consumption compared with the electrostatic-actuated MEM-tunable VCSEL.

To understand the wavelength tuning behaviour, we calculated the laser emission wavelength as a function of air-gap thickness for the designed NEMO-tunable VCSEL, as shown by the blue curves in Fig. 4. In principle, the wavelength-tuning range should be limited by the free-spectral range of the optical cavity ( $\sim 40$  nm), given that the air gap can be changed from 1.1 to 0.4  $\mu\text{m}$ . However, the reflection bandwidth of the HCG top mirror also varies as the air gap changes, because the air gap also contributes to the overall mirror reflectivity depending on its optical length<sup>25</sup>. Hence the measured wavelength tuning range of 18 nm is limited by the drop in the mirror reflectivity as the cavity wavelength detunes from the centre, which results in a higher threshold gain being required to achieve the lasing condition. This is in agreement with the observed increase of threshold current at both edges of the tuning spectrum shown in Fig. 3b. This wavelength limitation originates from the smaller reflection bandwidth of the HCG mirror (shown by the dotted white curve), because the present design is intentionally engineered to yield a large fabrication tolerance<sup>19</sup>. We anticipate that a larger wavelength tuning range of 35–40 nm can be attained by using an HCG top mirror designed to yield a much broader reflection bandwidth, so the wavelength tuning curve overlaps entirely within the highly reflective mirror bandwidth of the HCG as shown in Fig. 4.

The mechanical response of various NEMO structures was measured by applying a sinusoidal a.c. modulating voltage in

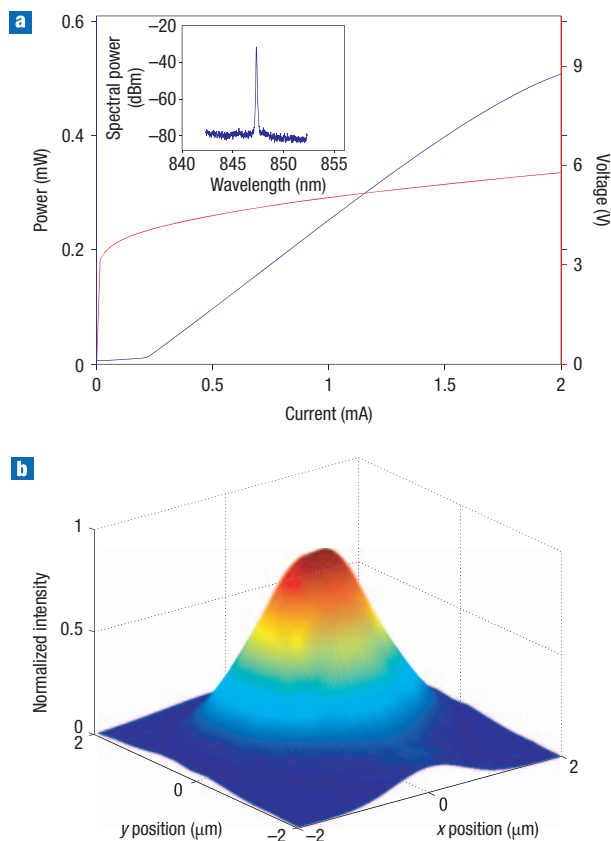


**Figure 2** Optical characteristic of NEMO-tunable VCSEL. **a**, Output light intensity (blue curve) and voltage (red curve) as a function of the input electric current, showing a very low threshold current of 200  $\mu$ A. The inset shows the measured single-mode optical emission spectra of the device with a  $>40$ -dB suppression of higher-order transverse modes. **b**, Measured optical near-field beam profile of the NEMO VCSEL with the mobile HCG top mirror.

addition to a d.c. voltage, while the VCSEL was injected with a constant current. The emission light was then collected by an optical fibre and sent to the optical spectrum analyser. As the signal integration time of an optical spectrum analyser is much slower compared with the voltage modulation, a spectrally broadened emission can be observed as the nanomechanical actuator (and hence the emission wavelength) is being modulated. The spectral broadening is directly proportional to the magnitude of the mechanical deflection, and the measured response of various NEMO structures is shown in Fig. 5a. Among the different nanomechanical structures, the membrane actuator exhibits the fastest mechanical resonant response with a 3-dB frequency bandwidth of 3.3 MHz, or equivalently the tuning speed of this device is calculated to be about 150 ns. Compared with existing DBR-based electrostatic-actuated MEM-tunable VCSELs, the demonstrated NEMO VCSEL with an integrated mobile HCG has a  $\sim 40$ – $50$  times faster wavelength tuning speed. The frequency response of the membrane structured actuator also exhibits a higher quality factor owing to higher mechanical stiffness. Damping is primarily due to air drag on the mechanical actuators, which can be reduced by properly packaging the devices.

A comparison of various mechanically tunable VCSEL technologies is shown in Fig. 5b, which shows the calculated tuning speed and actuating voltage as a function of the

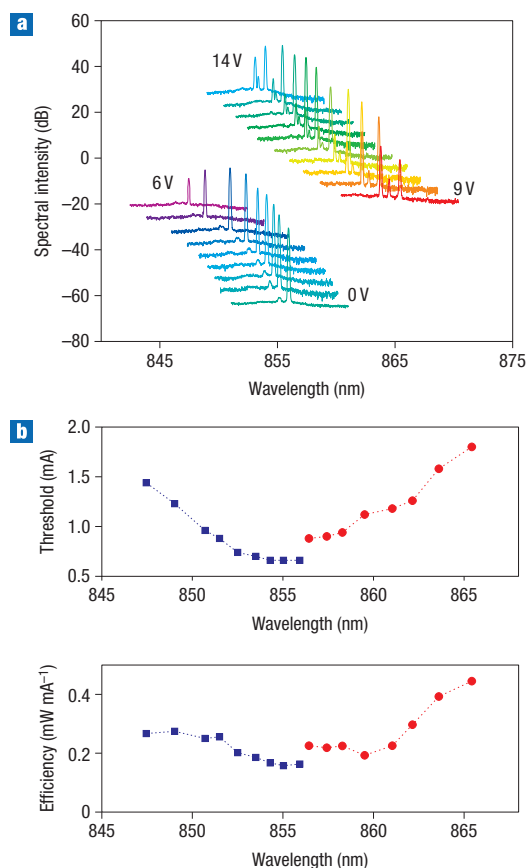


**Figure 3** Continuous wavelength tuning of NEMO-tunable VCSEL.

**a**, Measured continuous wavelength tuning spectra of the NEMO-tunable VCSEL with an 18-nm tuning range. **b**, Measured laser threshold current and slope efficiency of the NEMO-tunable VCSEL under the corresponding emission wavelengths.

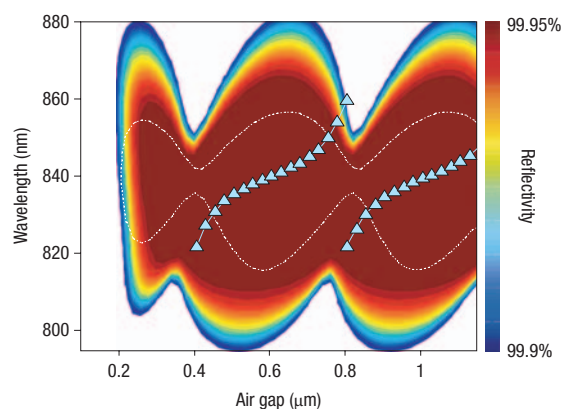


**Figure 4** Wavelength-tuning range limited by mirror bandwidth. Calculated laser emission wavelength (blue curves) and the HCG mirror reflection bandwidth (colour-coded contour) as a function of the air-gap thickness for a NEMO-tunable VCSEL designed to extend the wavelength tuning range to 35–40 nm. Shown in the dotted white curve is the  $>99.9\%$  reflection bandwidth for the present HCG design, illustrating that the wavelength range of 18 nm is limited by the smaller mirror bandwidth.



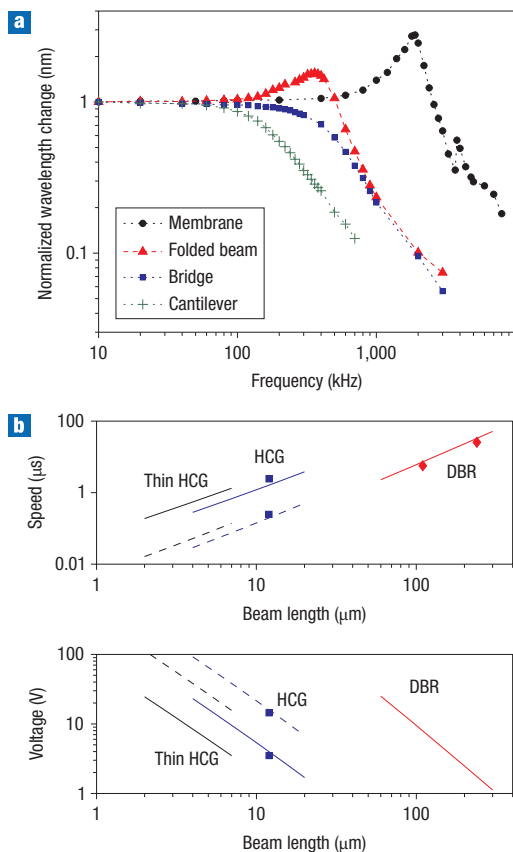


**Figure 5** Mechanical tuning speed of NEMO-tunable VCSEL. **a**, Measured mechanical response of various NEMO structures while modulating the nanomechanical actuators. **b**, Calculated tuning speed and voltage as a function of the mechanical beam length when using different mobile mirror designs (DBR, HCG and thin HCG) integrated with different mechanical actuators: cantilever (solid lines) and membrane (dashed lines). The thin HCG refers to the grating designed to strongly reflect TE polarized light, but the thickness is reduced by  $\sim 1/2$ . The dotted points are experimentally measured values from our fabricated NEMO devices (and earlier works).

mechanical beam length<sup>26</sup>. As an illustration, the tuning speed and voltage trade-off are calculated for two mechanical actuators: cantilever and membrane. Clearly, when scaling down the mechanical actuators, especially from the DBR microelectromechanical to HCG nanoelectromechanical mirror, a drastic improvement in tuning speed can be obtained while the required actuating voltage is also reduced. Furthermore, the HCG mirror presented here is designed to strongly reflect transverse-magnetic polarized light (electric field perpendicular to the gratings), but a similar concept can be applied to obtain a highly reflective mirror that operates for transverse-electric polarized light<sup>27,28</sup>. Because of the higher effective refractive index for the TE polarized light in a subwavelength grating structure<sup>29</sup>, the thickness required for the grating can be reduced by  $\sim 1/2$ . With such a thickness reduction, which enables further scaling down of the mechanical components, even faster tuning speeds to within tens of nanoseconds can be potentially achieved.

We demonstrate a high-speed nanoelectromechanical tunable laser by monolithically integrating a lightweight, single-layer HCG as the movable top mirror in a VCSEL. The small footprint of the HCG enables the scaling down of the mechanical actuating

components, which results in a drastic reduction in mass and substantial improvement in tuning speed. Using electrostatic actuation to control the air gap below the HCG, a compact and efficient tunable semiconductor laser with precise and continuous wavelength tuning is demonstrated with very fast tuning speed and ultralow power consumption. The simplicity, wavelength scalability and versatility of the single-layer HCG results in an elegant and attractive optical mirror design for the next generation of NEMO-tunable devices.

## METHODS

The epitaxy design of the NEMO-tunable VCSEL consists of the following components. The bottom, silicon-doped DBR is composed of 34 pairs of  $\text{Al}_{0.12}\text{Ga}_{0.88}\text{As}/\text{Al}_{0.9}\text{Ga}_{0.1}\text{As}$ . The nominally undoped, one-lambda cavity contains three 6-nm GaAs quantum wells surrounded by 8-nm  $\text{Al}_{0.3}\text{Ga}_{0.7}\text{As}$  barriers and sandwiched by an  $\text{Al}_{0.6}\text{Ga}_{0.4}\text{As}$  cladding layer. To provide current injection into the active region, two pairs of carbon-doped  $\text{Al}_{0.12}\text{Ga}_{0.88}\text{As}/\text{Al}_{0.9}\text{Ga}_{0.1}\text{As}$  are used immediately above the active region. Within that, 30-nm  $\text{Al}_{0.98}\text{Ga}_{0.02}\text{As}$  is used as the thermal oxidation layer. Above the current injection layer is a 1.1- $\mu\text{m}$  undoped GaAs sacrificial layer and a 235-nm silicon-doped  $\text{Al}_{0.6}\text{Ga}_{0.4}\text{As}$  HCG layer.

The structure of the HCG consists of periodic stripes of  $\text{Al}_{0.6}\text{Ga}_{0.4}\text{As}$  that are freely suspended, with air acting as the low-index cladding layers on the top and bottom. The grating is designed with the following parameters: period = 0.375  $\mu\text{m}$ , thickness = 0.235  $\mu\text{m}$ , duty cycle (DC) = 62%, air-gap thickness = 1.1  $\mu\text{m}$  ( $5\lambda/4$ ) where  $\lambda$  is the wavelength. The DC is defined as the ratio of the width of the high-index material to the grating period, and hence the width of the gap between the grating, or equivalently the critical lithography dimension, is 140 nm. Taking into account etching of the side-walls, the fabricated grating critical dimension is smaller ( $\sim 100$  nm). The HCG has an area of  $12 \times 12 \mu\text{m}^2$ , or equivalently 31 periods of  $\text{Al}_{0.6}\text{Ga}_{0.4}\text{As}$  grating stripes (0.26  $\mu\text{m}$  wide, 12  $\mu\text{m}$  long and 0.23  $\mu\text{m}$  thick) suspended above the air gap.

The fabrication process begins with mesa formation ( $\sim 100 \mu\text{m}$ ) by etching down to the bottom DBRs and is followed by thermal oxidation to form the oxide aperture ( $\sim 3 \mu\text{m}$ ). The next steps are the top- and back-side contact metal depositions. A part of the mesa is then etched to expose the p-doped current injection layer, on top of which the laser contact metal is deposited. Finally, the HCG is patterned by electron-beam lithography on polymethylmethacrylate (PMMA) photoresist and etched by reactive ion etching, where the HCG is aligned to the centre of the device mesa (oxide aperture) with  $\sim 1 \mu\text{m}$  accuracy. A wet chemical-based selective etching followed by critical point drying is required to remove the sacrificial material under the HCG layer and form the freely suspended grating structure, which is supported by nanomechanical beams.

Received 26 September 2007; accepted 17 January 2008; published 24 February 2008.

## References

- Horowitz, P. & Hill, W. *The Art of Electronics* (Cambridge Univ. Press, New York, 1980).
- Ilic, B. R., Krylov, S., Kondratovich, M. & Craighead, H. G. Optically actuated nanoelectromechanical oscillators. *IEEE J. Sel. Top. Quant. Electron.* **13**, 392–399 (2007).
- Bruce, E. Tunable lasers. *IEEE Spectrum* **39**, 35–39 (2002).
- Coldren, L. A. Monolithic tunable diode lasers. *IEEE J. Sel. Top. Quant. Electron.* **6**, 988–999 (2000).
- Craighead, H. G. Nanoelectromechanical systems. *Science* **290**, 1532–1535 (2000).
- Li, M., Tang, H. X. & Roukes, M. L. Ultra-sensitive NEMS-based cantilevers for sensing, scanned probe and very high-frequency applications. *Nature Nanotech.* **2**, 114–120 (2007).
- Cooper, M. A. Optical biosensors in drug discovery. *Nature Rev. Drug Discov.* **1**, 515–528 (2002).
- Lackner, M. et al. CO and CO<sub>2</sub> spectroscopy using a 60 nm broadband tunable MEMS-VCSEL at 1.55  $\mu\text{m}$ . *Opt. Lett.* **31**, 3170–3172 (2006).
- Knappe, S. et al. A chip-scale atomic clock based on <sup>87</sup>Rb with improved frequency stability. *Opt. Express* **13**, 1249–1253 (2005).
- Van Kessel, P. F., Hornbeck, L. J., Meier, R. E. & Douglass, M. R. A MEMS-based projection display. *Proc. IEEE* **86**, 1687–1704 (1998).
- Solgaard, O., Sandejas, F. S. A. & Bloom, D. M. Deformable grating optical modulator. *Opt. Lett.* **17**, 688–690 (1992).
- Wu, M. C., Solgaard, O. & Ford, J. E. Optical MEMS for lightwave communication. *J. Lightwave Technol.* **24**, 4433–4454 (2006).
- Iga, K. Surface-emitting laser — its birth and generation of new optoelectronics field. *IEEE J. Sel. Top. Quant. Electron.* **6**, 1201–1215 (2000).
- Koyama, F. Recent advances of VCSEL photonics. *J. Lightwave Technol.* **24**, 4502–4513 (2006).
- Chang-Hasnain, C. J. Tunable VCSEL. *IEEE J. Sel. Top. Quant. Electron.* **6**, 978–987 (2000).
- Harris, J. S. Jr. Tunable long-wavelength vertical-cavity lasers: The engine of next generation optical networks? *IEEE J. Sel. Top. Quant. Electron.* **6**, 1145–1160 (2000).
- Riemenschneider, F. et al. Continuously tunable long-wavelength MEMS-VCSEL with over 40-nm tuning range. *IEEE Photon. Technol. Lett.* **16**, 2212–2214 (2004).

18. Hofmann, W. *et al.* High speed ( $>11$  GHz) modulation of BCB-passivated  $1.55\ \mu\text{m}$  InGaAlAs-InP VCSELs. *Electron. Lett.* **42**, 976–977 (2006).
19. Huang, M. C. Y., Zhou, Y. & Chang-Hasnain, C. J. A surface-emitting laser incorporating a high-index-contrast subwavelength grating. *Nature Photon.* **1**, 119–122 (2007).
20. Huang, M. C. Y., Zhou, Y. & Chang-Hasnain, C. J. Nano electro-mechanical optoelectronic tunable VCSEL. *Opt. Express* **15**, 1222–1227 (2007).
21. Mateus, C. F. R., Huang, M. C. Y., Deng, Y., Neureuther, A. R. & Chang-Hasnain, C. J. Ultrabroadband mirror using low-index clad subwavelength grating. *IEEE Photon. Technol. Lett.* **16**, 518–520 (2004).
22. Mateus, C. F. R., Huang, M. C. Y., Chen, L., Chang-Hasnain, C. J. & Suzuki, Y. Broad-band mirror ( $1.12\text{--}1.62\ \mu\text{m}$ ) using a subwavelength grating. *IEEE Photon. Technol. Lett.* **16**, 1676–1678 (2004).
23. Huang, M. C. Y., Cheng, K. B., Zhou, Y., Pisano, A. P. & Chang-Hasnain, C. J. Monolithic integrated piezoelectric MEMS-tunable VCSEL. *IEEE J. Sel. Top. Quant. Electron.* **13**, 374–380 (2007).
24. Bendickson, J. M., Glytsis, E. N., Gaylord, T. K. & Brundrett, D. L. Guided-mode resonant subwavelength gratings: Effects of finite beams and finite gratings. *J. Opt. Soc. Am. A* **18**, 1912–1928 (2001).
25. Maute, M. *et al.* Long-wavelength tunable vertical-cavity surface-emitting lasers and the influence of coupled cavities. *Opt. Express* **13**, 8008–8014 (2005).
26. Mateus, C. F. R., Huang, M. C. Y. & Chang-Hasnain, C. J. Micromechanical tunable optical filters: General design rules for wavelengths from near-IR up to  $10\ \mu\text{m}$ . *Sens. Actuat. A* **119**, 57–62 (2005).
27. Ding, Y. & Magnusson, R. Resonant leaky-mode spectral-band engineering and device applications. *Opt. Express* **12**, 5661–5674 (2004).
28. Boutami, S., Benbakir, B., Leclercq, J. L. & Viktorovitch, P. Compact and polarization controlled  $1.55\ \mu\text{m}$  vertical-cavity surface-emitting laser using single-layer photonic crystal mirror. *Appl. Phys. Lett.* **91**, 071105 (2007).
29. Gustavsson, J. S. *et al.* Efficient and individually controllable mechanisms for mode and polarization selection in VCSELs, based on a common, localized, sub-wavelength surface grating. *Opt. Express* **13**, 6626–6634 (2005).

### Acknowledgements

This project was supported by the Defense Advanced Research Projects Agency (DARPA) Center for Optoelectronic Nanostructure Semiconductor Research and Technology (CONSRT). We thank Land Mark Optoelectronic for the growth of the epitaxy wafer and Berkeley Microfabrication Laboratory for the fabrication support.

Correspondence and requests for materials should be sent to C.C.H.

Reprints and permission information is available online at <http://npg.nature.com/reprintsandpermissions/>